Microprocessors and Microsystems 76 (2020) 103079

Contents lists available at ScienceDirect

Microprocessors and Microsystems

journal homepage: www.elsevier.com/locate/micpro

Intelligent fault diagnosis in microprocessor systems for vibration analysis in roller bearings in whirlpool turbine generators real time processor applications

L. Mubaraali [a,*], N. Kuppuswamy [b], R. Muthukumar [c]

[a] Research Scholar, Faculty of ICE, Anna University, India
[b] Professor and Dean Mechanical Engineering KIT, Coimbatore, 641402, India
[c] Associate professor and Electrical and Electronics Engineering ESEC, Erode, 638057, India

ARTICLE INFO

Article history:
Received 13 December 2019
Revised 10 February 2020
Accepted 3 March 2020
Available online 4 March 2020

Keywords:
Microprocessor
Condition monitoring
Fault diagnosis
Feature extraction
Signal denoising
Vibration measurement

ABSTRACT

Large steam turbines used for electrical power generation demand governing systems of very high integrity (safety) and availability. The latest generation of electronic governors uses microprocessors in a distributed, two level architecture to achieve the required integrity and availability and in addition provides greater configuration flexibilities and wider facilities than earlier governors. Rolling element bearings are one of the major machinery components used in industries like power plants, chemical plants and automotive industries that require precise and efficient performance. Vibration monitoring and analysis is useful tool in the field of predictive maintenance in small hydro electric power plants. Health of rolling element bearings can be easily identified using vibration monitoring because vibration signature reveals important information about the fault development within them. Numbers of vibration analysis techniques are being used to diagnosis of rolling element bearings faults. This paper proposes a new signal feature extraction and fault diagnosis method for fault diagnosis of low-speed machinery. Initially, the proposed work explores the Continuous Wavelet Transform (CWT) to adaptively remove the exact noises from vibration analysis and then feature extraction is performed by exploiting the noise removed pre-processed data. Statistic filter (SF) and Hilbert transform (HT) are combined with moving-peak-hold method (M-PH) to extract features of a fault signal, and Special bearing diagnostic symptom parameters (SSPs) in a frequency domain that are sensitive to bearing fault diagnosis are defined to recognize fault types. The SF is first used to adaptively cancel noises, and then fault detection is performed by exploiting the optimum symptom parameters in a time domain to identify a normal or fault state. For precise diagnosis, the SSPs are calculated after the signals are processed by M-PH and HT.

1. Introduction

The evolution of microprocessor architecture depends upon the changing aspects of technology. As die density and speed increase, memory and program behaviour become increasingly important in defining architecture tradeoffs. While technology enables increasingly complex processor implementations, there are physical and program behaviour limits to the usefulness of this complexity. Physical limits include device limits as well as practical limits on power and cost A Whirlpool turbine generator plays an irreplaceable role in modern power industry. Over the past decades, the safety of equipment has received more and more attention and the fault diagnosis of rotary machinery has become a hot research topic. Faults not only include the imbalance of the rotor itself but also may occur at the bearings, gear boxes and couplings, which determines the variation and complexity of faults. Hence, how to describe faults is key to fault diagnosis. Various sources such as vibration [1], electric current and acoustic signals [2,3] are used in diagnosis. Generally, vibration signals are important sources of faults and contain abundant information about running states of rotary machinery, which are widely used to extracted features in fault description.

Fault diagnosis and estimation has been done using different techniques in different domains [4]. Bearing faults have been diagnosed mostly using techniques, which diagnose bearing defects by analyzing different types of signals, such as the vibration acceleration signal of a bearing's housing measured through accelerometers [5], the stator current of the induction motor [6], the acoustic emission (AE) signals [7], and the stray flux spectra [8]. Tech-

* Corresponding author.
E-mail address: imubaraali@gmail.com (L. Mubaraali).

https://doi.org/10.1016/j.micpro.2020.103079
0141-9331/

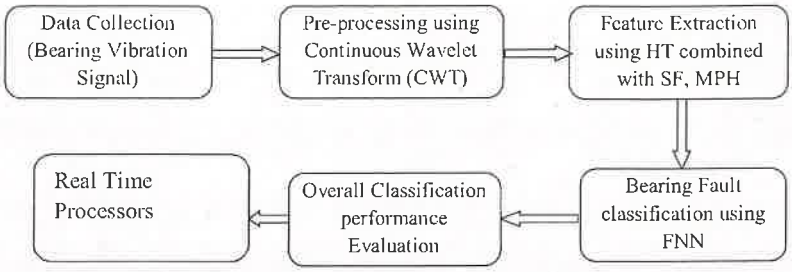

Fig. 1. Proposed block diagram.

niques that analyze the vibration acceleration signal and the motor stator current are effective in diagnosing bearing defects at high rotational speeds. However, at low rotational speeds, bearing defects, especially incipient defects, are more effectively diagnosed using AE-based methods, as they are sensitive to the low energy acoustic emissions released by a developing crack in the bearing even if it is sub-surface [9]. Hence, in this paper, AE signals are used to diagnose incipient bearing defects under variable operating speeds. The diagnosis of bearing defects under variable operating speeds is an important problem. Many studies [10] have considered similar problems in different contexts. For instance, the authors of [11] have studied the application of traditional vibration-based techniques for the diagnosis of various rotor faults in machines operating at different speeds and with different foundation supports.

AE-based methods mostly diagnose bearing defects either by using envelope analysis [12], or by constructing discriminative models for features extracted from the bearing fault signals using discriminative classifiers such as support vector machines (SVM) [13]. Envelope analysis-based methods diagnose bearing defects by looking for peaks at characteristic frequencies associated with each defect type in the power spectrum of the envelope signal. However, these characteristic defect frequencies (CDFs) are functions of the bearing's rotational speed, which renders these techniques ineffective under variable operating speeds. Similarly, feature extraction-based methods are also not effective in diagnosing bearing defects under variable operating speeds, as variations in the operating speed result in inconsistent features that yield poor discriminative models. Hence, these methods have predominantly been used to diagnose bearing defects under constant operating speeds. Moreover, since feature extraction-based methods use the statistical properties of the time and frequency domain AE signal, and the complex envelope signal; the diagnostic performance of these methods depends upon the quality of the extracted features. The selection of appropriate features requires both expert domain knowledge and feature selection algorithms to eliminate redundant and irrelevant features [13]. In summary, so far, the literature on the application of vibration or AE analysis to automatically diagnose lowspeed bearing fault has not been found.

This work carries out the automatic diagnosis of low-speed bearings using vibration analysis, which has widely been used in production plants at a low cost. The motivation of the work is as follows.

1) In order to automatically extract the weak fault signal of a low-speed bearing from the vibration signal contaminated by strong noises, the self-adaptive signal processing methods based on M-PH, SF, and HT are proposed [14]. Also before that, a pre-processing process is carried out using Continuous Wavelet transform to remove the false signal from the data samples.
2) In order to sensitively reflect the features of the extracted fault signal, the special bearing diagnostic SPs (SSPs) are newly defined for precision diagnosis [15].
3) In order to precisely and automatically determine the fault type of low-speed bearings, the construction method for the intelligent diagnostic system is proposed by introducing fuzzy neural network with the use of the SPs in time and frequency domain. The design of FNN includes the development of the fuzzy rules that have IF-THEN form [16].

The fault states of a bearing can be classified into early stage (spot flaw), middle stage (multiple localized defects), and final stage (generalized defects) [17]. This paper emphasizes early fault diagnosis, which is beneficial in real-world industries, because potential catastrophic failure can be prevented by successful early fault detection [18]. In condition-based maintenance, early fault detection can also provide important information to carry out the state trend control [19]. The focus of this paper is early fault diagnosis of the roller bearing at low speeds, but the bearing diagnosis method will be tested during the middle and final stages in a forthcoming study [20].

2. Proposed methodology

The method proposed in this paper includes a training procedure and a diagnostic procedure [21]. The overall proposed methodology flow diagram for low speed bearings is shown in Fig. 1. In fact, these systems must have a high degree of reliability and availability to remain functional in specified operating conditions without needing expensive maintenance works. Especially for offshore plants, a clear conflict exists between ensuring a high degree of availability and reducing costly maintenance

The training procedure requires signals from the equipment while operating in a normal state and each abnormal state [22]. The main purpose of training is to establish the diagnostic rules by FNN, which includes the rules for the condition survey and the rules for precise diagnosis. In the diagnostic procedure, SPs of the diagnostic signal are calculated, and the state of the bearing is determined using the rules obtained in the training step [23]. The diagnostic procedure also includes the condition survey step and the precise diagnostic step.

Three typical bearing faults—the inner race flaw, outer race flaw, and roller flaw—are utilized here to demonstrate the efficacy of the proposed method. There is no universally accepted definition of "low-speed rotating machinery," but the term typically refers to machines operating at a shaft rotational speed below 600 rpm or in a range from 0.33 to 10 Hz [24]. In this paper, fault diagnosis experiments for low-speed bearings in a real rotating machine were conducted to verify the performance of the method with vibration speed measurements taken from 40 to 200 rpm.

1) Noisecanceling: In our previously published paper, a lot of environmental noises can be cancelled self-adaptively using SF for fault diagnosis of middle and high-speed rotating machinery. Details regarding the basic theory and advantages of SF can be found in [25]. However, during the operation of low-speed

equipment, environmental noises are complex and are significantly affected by the operating conditions, such as speed and load. Therefore, it is important to cancel the noises as cleanly as possible in vibration-based fault diagnosis by multiple feature extraction method. Peak-hold-down sample (PHDS) and HT are suitable for processing signals with a low SNR. The traditional PHDS is an effective down sampling method, but the signal sampling frequency will decrease after processing by PHDS. Since this paper combines PHDS with HT to extract features of bearings rotating at a low-speed, a relatively high sampling frequency of the signal is required. For this reason, an M-PH is proposed after processing by which the sampling frequency will not change. In this paper, the HT is combined with M-PH to extract the fault signal.

2) Symptom parameters (SPs): In addition, because intelligent diagnosis systems based on a computer cannot determine the fault type like the expert by "observing the spectrum," it is necessary to use SPs for automatic diagnosis. When taking the practicability into consideration, SPs used in the condition survey are traditional parameters, which have a good effect on quickly judging if the state of equipment is normal or abnormal. In the precise diagnosis step, in order to effectively reduce the influence of noises and extract fault features, the special bearing diagnostic SPs (SSPs) are defined for roller bearing fault diagnosis of low-speed rotating machines.

2.1. Pre-processing of using CWT

The CWT is thus a natural tool to be used early in the investigation of the properties of signals to develop processing algorithms and concepts. It produces a representation of the time-frequency features of the signal, with the additional benefit of a so-called "zooming" effect. This zooming effect modifies the spectral resolution to be a function of scale—the small-scale structure has higher resolution (frequency bandwidth) than does large-scale structure. In other words, the CWT zooms in to display detailed, fine features (high frequency) and zooms out to display large, coarse trends (low frequency). Thus, for signals for which spectral characteristics or statistical properties are likely to change over time, the CWT could be used to identify those signal features that are potentially exploitable by signal processing.

In this work, CWT the signals are analyzed using a set of basis function, which are related to each other by simple scaling and translation. CWT is a wavelet transform with a continuous mother wavelet, continuous dilation parameter, and a discrete translation parameter. A wavelet transform is a convolution of the wavelet function $\Psi(t)$ with the signal $x(t)$. Continuous wavelet transform (CWT) of a continuous square integrable function $x(t)$ at a scale a>o and b belongs to R is expressed by the following integral.

$$X_{\omega}(a,b) = 1^{1/\sqrt{a}}1 \int_{-\alpha}^{\alpha} x(t)\Psi^{*}\left(\frac{t-b}{a}\right)dt \tag{1}$$

where $1/\sqrt{a}$ is the normalization factor and $\Psi^{*}(\frac{t-b}{a})$ is the conjugate of the mother wavelet function [26]. The following preprocessing steps to remove the noise are

(1) Decomposition: Choose a wavelet, and choose a level N.Compute the wavelet decomposition at level N.
(2) Thresholding: For each level from 1 to N, select a threshold and apply soft or hard thresholding to the detailed coefficients.
(3) Reconstruction: After decomposition thresholding is applied to detail coefficients and after that signal is reconstructed by using original approximate coefficients and modified detail coefficients.

A noisy signal data collection is taken as an input. From the input noisy signal "x_{noisy}", the standard deviation or the Median absolute deviation can be calculated by the formula $\sigma = std(x_{noisy})$ or $\sigma = mad(x_{noisy})/0.6745$ respectively which gives an approximate estimation of the noise level of the noisy signal "xnoisy".In this paper, Median absolute deviation the is calculated for evaluation of the threshold the d value. One of the first methods for selection of threshold was developed by Donoho and Johnstone [27] and it is called as universal threshold. It is given by Threshold, $T = \sigma$ where N denotes the no. of data samples of the noisy signal

Thresholding is an important step in removing noise from a noisy signal. Hard thresholding and Soft thresholding are the two common and most popular methods. The CWT coefficients, "C" of the noisy signal is shrunk by the thresholding algorithm [27] given below.

$$\begin{matrix} New\,Coefficients = C - sign(C) \times T & IF|C|^3 > T = 0 \\ Otherwise & 0 \end{matrix} \tag{2}$$

In this thresholding algorithm, the CWT coefficients, "C" to the power three which are smaller than the threshold value, "T" is set to zero otherwise coefficients are shrunk in magnitude according to the above formula. The CWT coefficients computed are available in a matrix form. The number of columns in the matrix is equal to the signal length while the number of rows is 24, since the computation is done for scales from $m = 6$ to 29. Thus in this work, the above thresholding algorithm was applied to each element of the CWT coefficient matrix. Finally, the inverse CWT of the thresholded CWT matrix was computed by convolving with the Morlet wavelet (as was done for forwarding CWT computation) at same scales and performing a weighted summation across scales.

2.2. Feature selection of fault signal using M-PH, SF, and Hilbert transform (HT)

Features are some representative's values which can indicate bearing conditions. The represented features include time domain features such as mean, root mean squares (RMS), variance, skewness, kurtosis, etc., frequency domain features such as content at the feature frequency, the amplitude of FFT spectrum, etc., and time-frequency domain features such as statistical characteristics of short time Fourier Transform (STFT), Wigner–Viller distribution, wavelet transform, etc.

In this study, there are features like mean, rms, shape factor, skewness, kurtosis, crest factor, entropy estimation value, entropy estimation error, histogram upper bound, histogram lower bound, rms frequency, frequency center value, root variance frequency value, and first 8 order coefficients of the auto-regression (AR) model are extracted from the vibration signal. All the features extracted were computed from each bearing measurement using MATLAB code. Therefore it was obtained a 90 by 21 feature matrix. These features are extracted using the proposed Transform and it would be fed to the proposed Fuzzy Neural Network (FNN) classifier model for bearing fault classification.

2.3. Moving-Peak-Hold (M-PH) method for refining peak signal characteristics

Low-speed rotating machinery diagnosis is challenging, as described above due to the difficulty in extracting the fault signal from the diagnostic signal contaminated by noises. Effective feature extraction is the key to processing raw vibration data. The down sampling approach is, as of now, the only effective method for feature extraction for the purposes of low speed bearings diagnosis. The PHDS algorithm is a simple and effective peak holding and down sampling method originally proposed by Noda [28] for

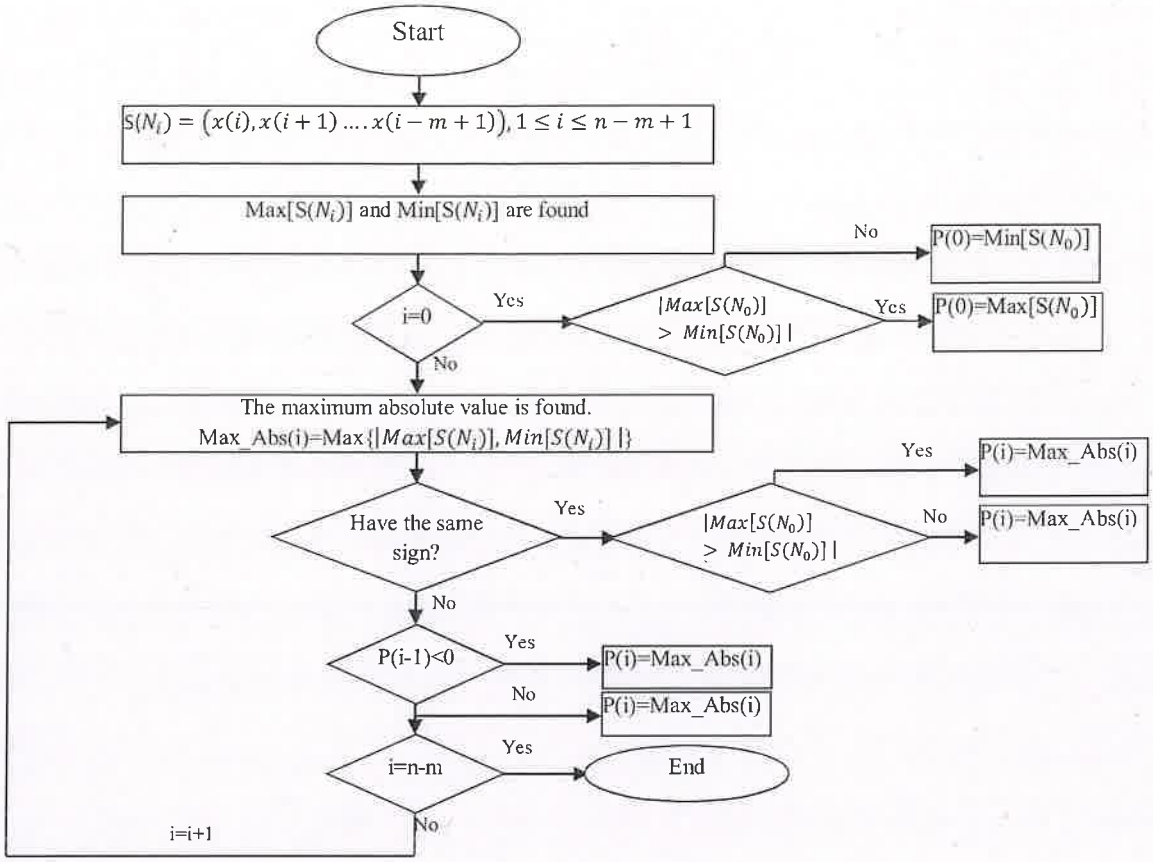

Fig. 2. Flowchart of M-PH.

feature extraction to detect rotor problems. It is useful for monitoring the conditions of low-speed rotary components based on the vibration and AE signals, even at a 500-Hz down sampling ratio [28].

M-PH retains the advantages of PHDS in refining peak signal characteristics, by which the information at low frequencies can be extracted according to the moving average method. The value of each point is redefined by PHDS, which acquires the necessary information during the feature extraction process. A flowchart of the M-PH method is shown in Fig. 2. As an example, the outer race fault signal of a roller bearing was processed by PHDS and M-PH, respectively, and then HT was conducted to further extract the signal feature. The waveform of PHDS was not providing the proper features due to a relatively low sampling frequency. Whereas, the spectrum of the signal processed by M-PH exhibited peaks at the pass frequency and its high-order harmonics.

Each data segment with a fixed number of data points is analyzed by M-PH to extract the signal characteristics in the same way as the moving average method. As shown in Fig. 2, when the ratio is m, each segment with m points of signal x is analyzed, respectively. For example, when the *i*th segment is analyzed, the maximum (Max [S(Ni)]) and minimum (Min [S (Ni)]) from this segment are picked out first. Then, it is judged whether the maximum and minimum signs are the same. At this point, the new value is determined according to the following situations. Max_Abs (i) is the larger absolute value between Min [S (Ni)] and Max [S (Ni)]. If the maximum and minimum signs are the same, Max_Abs (i) or its inverse is used to replace the value of this point according to this sign for this segment. If the signs are different, Max_Abs (i) or its inverse is used to replace the value of this point according to the sign of the previous datum. The purpose of this method is to highlight the peak characteristics of the signal as clearly as possible.

2.4. Hilbert transform (HT) for signal decomposition

Hence the vibration signals are pre-treated via M-PH, and then the signals are decomposed via Hilbert transform (HT) to extract and reconstruct the feature spectra for distinguishing states. In order to characterize the flaws from vibration signals, it is necessary to acquire the signals by deliberately introducing defects in the machines are considered. From the time domain analysis of the signals, it is found that frequency is different for volumetric and planar defect hence it is necessary to obtain the frequency spectrum of the signals in order to analyze the flaws. Next step is to identify an appropriate transform for converting the time domain into the frequency domain. From the literature, Fourier transform is the highly reliable tool for converting a time domain signal into a frequency domain. However as the ultrasonic test signals are non-stationary in nature, frequency transform could not provide the desired results. Hence Hilbert Transform is chosen for the analysis. Hilbert Transform performs the decomposition of the input signal by removing the high-frequency components. These high-frequency components are called Intrinsic Mode Function. This process is repeated until the below condition is satisfied.

1. The number of local extreme of and the number of its zero-crossings must either be equal or differ at most by one.
2. At any time t, the mean value of the "upper envelope" (determined by the local maxima) and the "lower envelope" (determined by the local minima) is zero. The HT transform steps are as follows

The Hilbert transform is an important tool in constructing analytic signals for various purposes, such as obtaining the envelope of a signal in instantaneous frequency analysis, amplitude modulation, signal demodulation, and many other domains. There are

many ways to define the Hilbert transform meaningfully. Suppose we have a signal x(t), the conventional Hilbert transform of a continuous signal x(t) is computed as

$$\hat{x}(t) = \frac{1}{\pi} PV \int_{-\infty}^{\infty} \frac{x(\tau)}{t-\tau} d\tau \tag{3}$$

where $\hat{x}(t)$the Hilbert is transform and the Cauchy principle Value, PV is taken in the integral.

The continuous Hilbert transform consists of a $\pi/2$ rad phase shift (for positive frequencies only) in the frequency domain.T he Fourier transform of the Hilbert transform is given by [29]

$$\hat{X}(\omega) = -jsgn(\omega)X(\omega) \tag{4}$$

where

$$-jsgn(\omega) = \begin{cases} j, & for\ \omega > 0 \\ 0\ for\ \omega = 0 \\ -j, & for\ \omega < 0 \end{cases}$$

And X(ω) is the Fourier transform of x(t). The discrete Hilbert transform is developed as an exact equivalent of the Hilbert transform for discrete domain sequences and is defined as [29]

$$\hat{X}(n) = X(n) * h(n) \tag{5}$$

where h(n) is the impulse response of the discrete Hilbert transformer.

$$h(n) = \begin{cases} \frac{2\sin^2\left(\frac{\pi n}{2}\right)}{\pi n} & n \neq 0 \\ 0 & n = 0 \end{cases}$$

The transfer function of the discrete Hilbert transform is defined as

$$H(\omega) = \begin{cases} j, & 0 < \omega < \pi \\ 0, & \omega = 0 \& \ \omega = \pi \\ -j, & -\pi < \omega < 0 \end{cases}$$

The procedure to identify the components in the vibration signal spectrum related to the bearing faults relying on Hilbert transformation is as follows

Step 1: Compute the Fourier Transform of the Vibration of signal in the time domain to isolate the resonance of the system and to identify the largest harmonic component

Step 2: The vibration signal in the time domain is band-pass filtered in order to obtain a reduced spectrum around the largest harmonic component

Step 3: Compute the Hilbert transformation of the band-pass filtered signal.

Step 4: Compute the Fourier Transform of the analytical signal obtained through Hilbert transformation.

Hence the Feature selection process directly reduces the number of original features by selecting a subset of them that still that still retains sufficient information for classification. Usually, a large number of features often include many garbage features. Such features are not only useless in classification, but also sometimes degrade the performance of a classifier which is designed by a finite number of training samples. In such a case short, removing the garbage features can improve the classification accuracy.

2.5. Fault diagnosis using FNN

The features extracted from the vibration signals are used for classification and determining the action. The extracted features are given asan input signal to the FNN based classifier. The classifier based on the extracted features classifies the signals into the following three classes: decreases steady and increases. The design of FNN includes the development of the fuzzy rules that have IF-THEN form. This is implemented by dint of optimal definition of the premise and consequent parts of fuzzy IF-THEN rules for the classification system through training of fuzzy neural networks. In the paper, the Takagi-Sugeno-Kang (TSK) types of IF-THEN rules that have a fuzzy antecedent and crisp consequent parts are used. The TSK-type fuzzy system approximates the nonlinear system with linear systems and has the following form:

$$if\ x_1\ is\ the\ A_{1j}\ and\ x_2\ is\ A_{2j}\ and \ldots\ldots and\ x_m\ is\ A_{mj} \tag{6}$$

$$Then\ y_j\ is\ \sum_{i=1}^{m} a_{ij}x_i + b_j \tag{7}$$

Here, x_i and y_j are input and output signals of the system, respectively, $i = 1, \ldots, m$ is the number of input signals, and $j = 1, \ldots, r$ is the number of rules. A_{ij} are input fuzzy sets; b_j and $a_{ij}$are coefficients.

The structure of fuzzy neural networks used for the classification of the vibration signal is based on TSK-type fuzzy rules. The FNN consists of six layers. The first layer is used to distribute the x_i ($i = 1, \ldots, m$) input signals. The second layer includes membership functions. Here, each node represents one linguistic term. Here, for each input signal entering the system, the membership degree where input value belongs to a fuzzy set is calculated. In the paper, the Gaussian membership function is used to describe linguistic terms

$$\mu 1_j(x_i) = e^{-\frac{(x_i - c_{ij})^2}{\sigma_{ij}^2}},\ i = 1, \ldots,\ m,\ j = 1, \ldots r \tag{8}$$

where c_{ij} and σ_{ij} are centrethe and width of the Gaussian membership functions, respectively. $\mu 1_j(x_i)$ is membership function of the ??th input variable for the jth term. m is a number of input signals; r is a number of fuzzy rules (hidden neurons in the third layer).

The third layer is a rule layer. Here, the number of nodes is equal to the number of rules. Here, $R_1, R_2, \ldots, R_r$ represents the rules. The output signals of this layer are calculated using t-norm min (AND) operation:

$$\mu_j(x) = \prod_i \mu 1_j(x_i),\ i = 1, \ldots m,\ j = 1, \ldots r, \tag{9}$$

where Π is the min operation.

These $\mu_j(x)$ signals are input signals for the fifth layer.The fourth layer is a consequent layer. It includes n linear systems. Here, the values of rules output are determined as

$$y_j = \sum_{i=1}^{m} x_i \omega_{ij} + b_j \tag{10}$$

In the next fifth layer, the output signals of the third layer are multiplied by the output signals of the fourth layer. The output of jth node is calculated as

$$y1_j = \mu_j(x).y_j \tag{11}$$

In the sixth layer, the output signals of FNN are determined as

$$\mu_k = \frac{\sum_{j=1}^{r} \omega_{jk} y1_j}{\sum_{j=1}^{r} \mu_j(x)} \tag{12}$$

Here, μ_k are the output signals of FNN (?? = 1, . . ., ??). After calculating the output signal, the training of the network starts.

Hence Roller bearing fault case for instance, there are classified into early stage (spot flaw), middle stage (multiple localized defects), and final stage (generalized defects). To handle this above FNN classification using 10 fold cross validation approach is proposed. Finally in the diagnostic procedure, SPs of the diagnostic signal are calculated using the membership function and the state of the bearing is determined using the IF-THEN rules obtained.

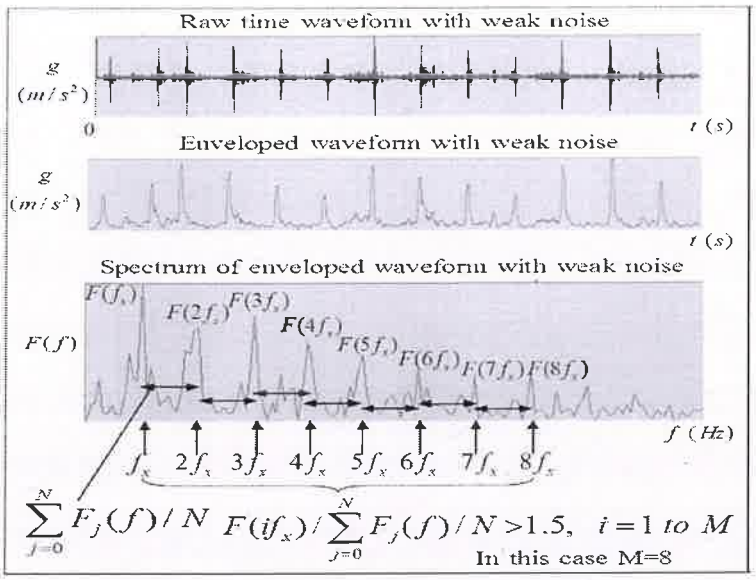

(a)

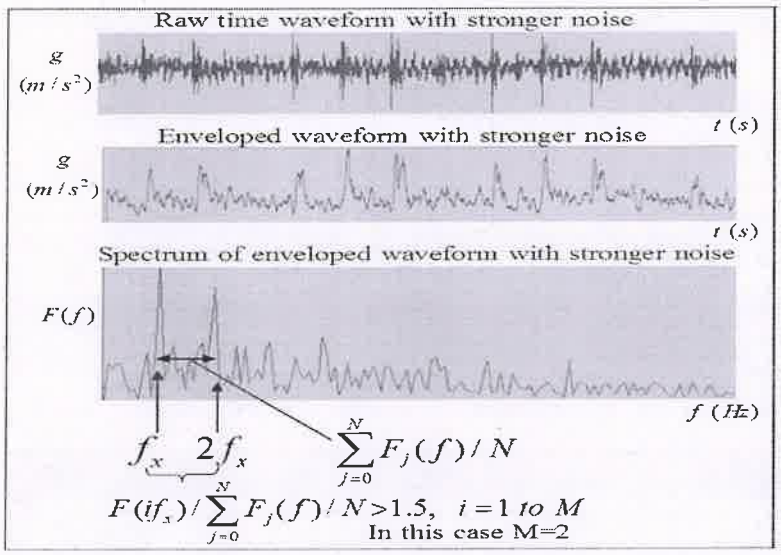

(b)

Fig. 3. Decision of high harmonic order M of pass frequency. (a) Raw data with weak noises. (b) Raw data with stronger noises.

2.5.1. Special SPs (SSPs)

The traditional time-domain SPs, such as peak value, RMS, crest factor, kurtosis, and skewness, are typically utilized for condition survey. However, they can only determine whether the bearing is in a normal or faulty state, and cannot judge particular fault types. Furthermore, because the *SNR* of the vibration signal is very small and the fault features of low speed bearing are not significant, other SPs must be found to detect the particular fault types. *SPFO, SPFR*, and *SPFI* defined in (8) and (9) serve this purpose here, and are applied to the fault type detection of low-speed bearings

$$if \frac{F(M.f_x)}{\sum_{j=1}^{N} \frac{F_j}{N}} > T_x \text{ then } M = M + 1 \tag{13}$$

$$SPF_x = \sum_{i=1}^{M} F(i.f_x) / \sum_{j=1}^{M.N} F_j \tag{14}$$

where M is the high harmonic order of pass frequency used to calculate SSPs, and can be determined by using the threshold T_x as shown in (8) and Fig. 3. f_x represents the pass frequency of one fault state; for example, f_0 represents the pass frequency of the outer race fault. T_x represents the threshold to identify the fault type when state x is identified, and set into 1.5 in this paper, as shown in Fig. 3. N is the number of points between the i th peak and the $(i-1)$ th peak, $F(if_x)$ is the amplitude of the enveloped spectrum at the frequency if_x, and $F_j(f)$ represents the amplitude of the enveloped spectrum at point j.

3. Experimental results

To verify the effectiveness of the proposed method, roller bearing fault detection experiments were conducted using a low-speed rotating machine with chain drive. Vibration signals were measured by an accelerometer located on top of the bearing hous-

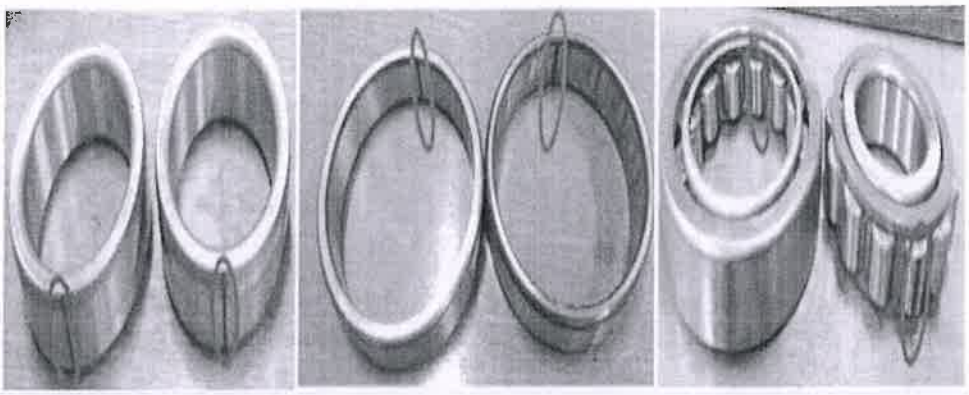

Fig. 4. Fault bearings used in the experiments. (a) IF fault, Small: 1.5 mm × 0.3 mm, Large: 2 mm × 0.3 mm, (b) OF fault, Small: 2.5 mm × 0.3 mm, Large: 4 mm × 0.5 mm, (c) RF fault, Small: 2 mm × 0.3 mm, Large: 4 mm × 0.5 mm.

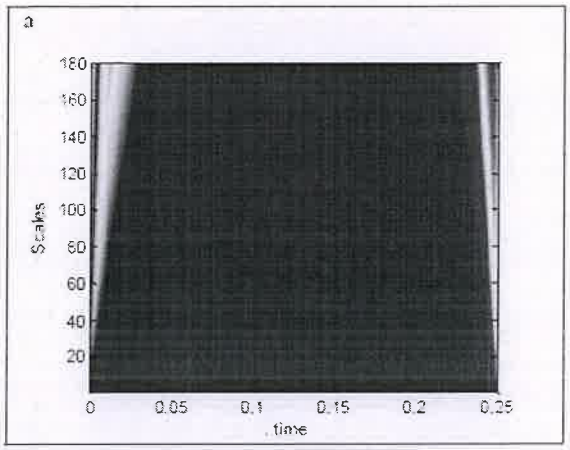

Fig. 5. (a) Healthy Bearing's CWT plot.

ing. The SAS12SC accelerometer (Fuji Ceramics Corporation) has 10.22 mv/ms^{-2} sensitivity in the measurement range from 5 Hz to 60 KHz. Bearing fault diagnosis focuses on the shape of the waveform and spectrum but not on acceleration value. No dimensional parameters (SSPs) were introduced to reflect the feature of the acceleration signals for the condition diagnosis. For this reason, in this paper, the signal unit from the accelerometer was presented in volts. In theory, roller bearing elements have their own specific rotational frequencies that appear in the enveloped spectrum when defects occur. These frequencies are referred to as defect frequencies (also referred to as "pass frequencies") [30]. The pass frequencies used in the experiments are shown in Table 1. The literature shows that upon fault of a roller bearing element, periodic pulses will appear in vibration signals.

Table 1
Passing frequencies of experimental bearing faults in turbine processors generators.

States of roller bearing	Pass Frequency (Hz)		
	40 rpm	100 rpm	150 rpm
Outer Race Fault	3.2	8.5	12.9
IF Fault	4.9	11.9	17.9
Roller Fault	3.4	8.8	11.1

The time interval of these pulses corresponds to the characteristic frequency. The pass frequencies of a defective bearing with two or more faults (scratches) on the same element are similar to those of a bearing with a single fault, but the characteristic parameters (e.g., RMS and kurtosis) increase as the bearing defects on the same element increase [31]. Based on these results, the fault detection of a bearing with a single fault is more difficult than fault detection of a defective bearing with two or more faults on the same element. In this paper, one fault per case was imposed for diagnosing the low speed roller bearing fault at an early stage. In all experiments, the sampling frequency was 100 kHz and the shaft ran at fixed speeds of 40, 50, 60, 70, 100, 150, and 200 rpm, respectively.

Four common bearing states were investigated: normal (N), fault on the outer race (OF), fault on the inner race (IF), and fault on the roller element (RF). The fault of each bearing is one line imposed by a wire cutting machine to simulate an early stage of fault. The imposed fault size was classified into "large" and "small" categories as per their dimensions (width and depth), as shown in Fig. 4.

3.1. Experimental results

A series of experiments was carried out to verify the effectiveness and feasibility of this method. The vibration signals were col-

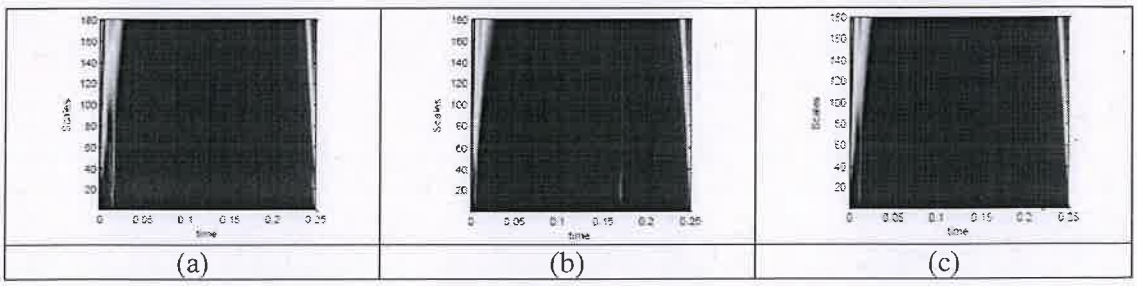

Fig. 6. Signal containing Inner Race Defects with different index of fault and its CWT plot.

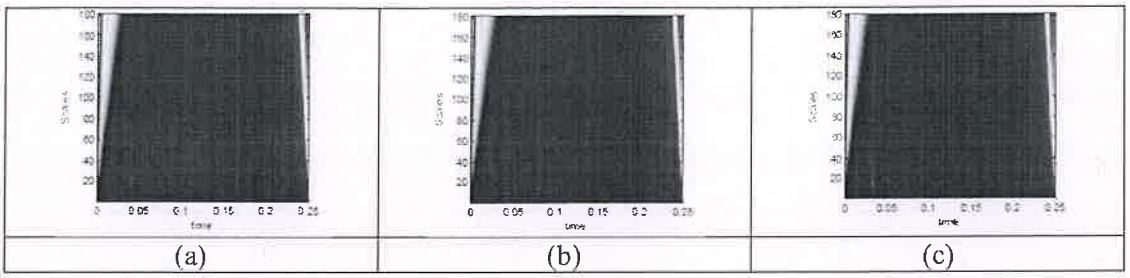

Fig. 7. Signal containing Outer race defect with different index of fault and its CWT plot.

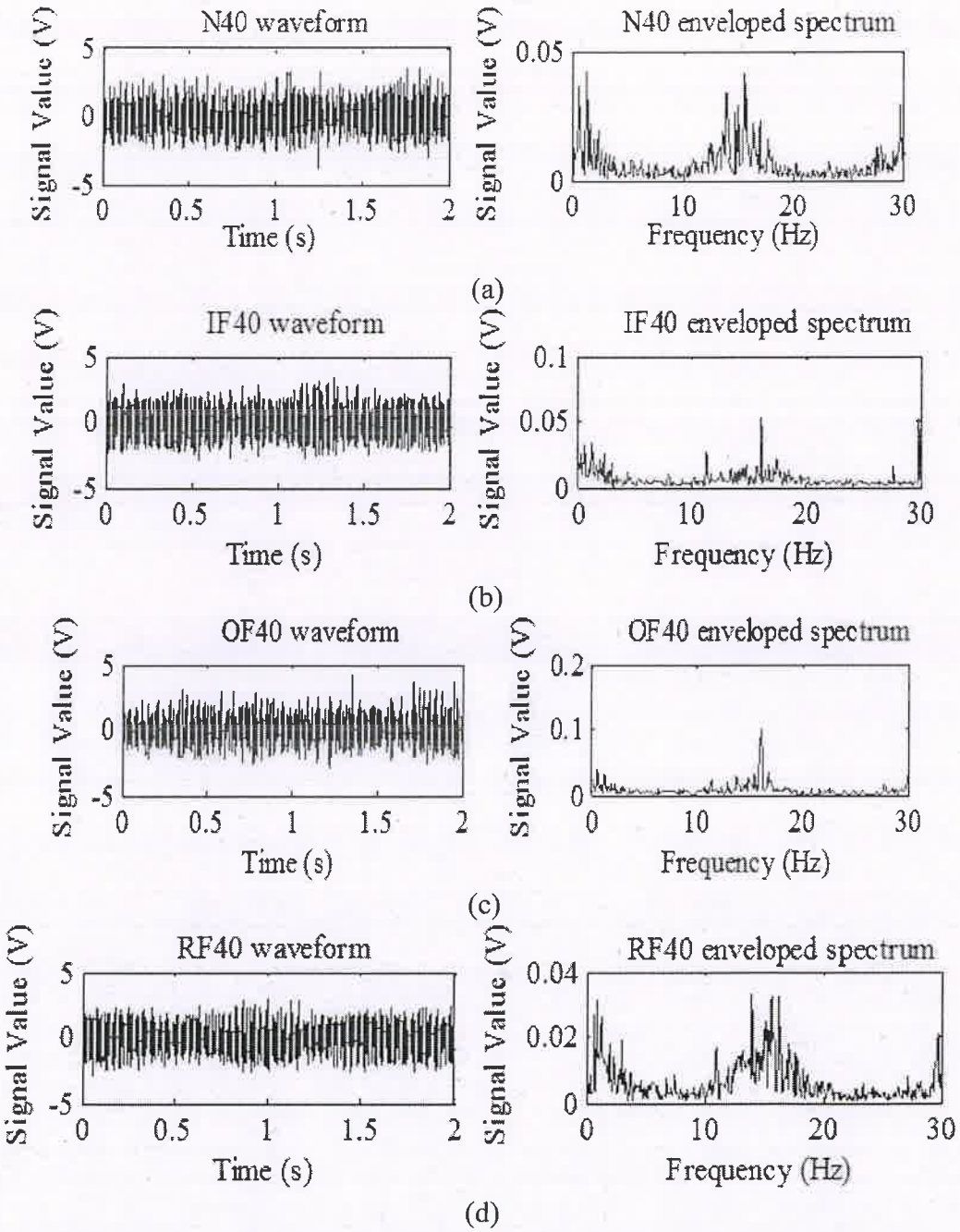

Fig. 8. Waveforms and enveloped spectra of the original signals at 40 rpm. (a) Normal state. (b) Inner race fault. (c) Outer race fault. (d) Roller fault.

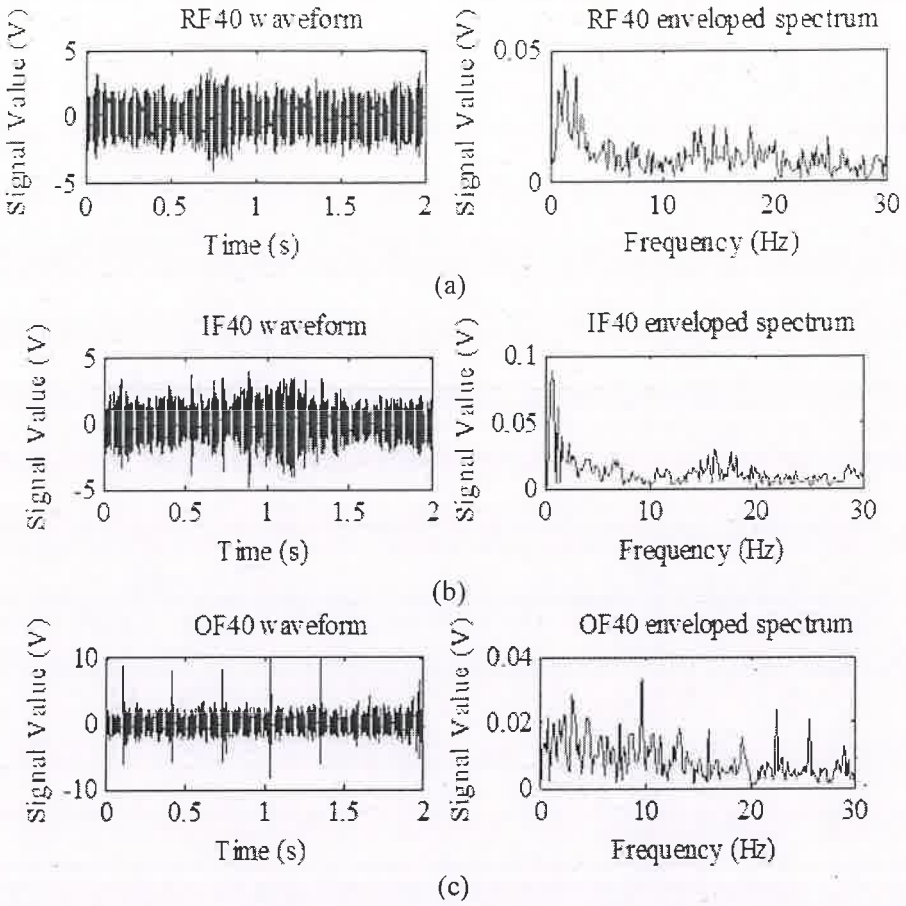

Fig. 9. Waveforms and enveloped spectra of fault signals processed by SF. (a) Roller element fault. (b) Inner race fault. (c) Outer race fault.

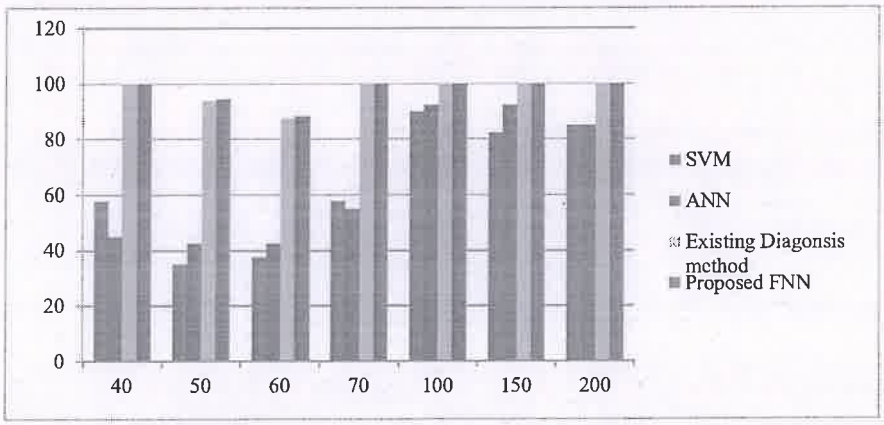

Fig. 10. Classification accuracy in processors with turbine generators.

lected from three different bearing conditions. Thirty data were collected from each bearing condition. Each data contains n sampling points. The n samples are pre-processed using CWT transform to remove noises from the vibration signal.

3.1.1. Results of pre-processing

The CWT plots for waveforms of healthy bearing, faulty inner race and outer races have been obtained using MATLAB and are shown from Figs. 5.a to 7.c. The CWT coefficients computed as above, form a matrix at the different scale and translation values; the higher value of coefficients suggest a high correlation (similarity) between the portion of the signal and that version of the wavelet. The colors in the plot show the relative values of the CWT coefficients. The light areas means higher values of the CWT coefficients and therefore, signal is very similar to the wavelet. Whereas, dark area means lower values of the CWT coefficients and it shows that the corresponding time and scale versions of the wavelet are dissimilar to the signal.

The data for bearing fault conditions were acquired from different loads. The time-domain plots and frequency plots of the raw vibration signals are shown in Fig. 8.

The selecting discrimination index of the SF used for these experiments was 1.25. The measured time of each sample was about 1.31 s (at 100-KHz sampling frequency), and the processing frequency band interval of the SF was about 5 Hz. For representing the effectiveness of the SF, the normalized waveform and en-

Table 2
Rule formation of FNN for 40 rpm.

S.no	FNN Rules	Faults
1	IF Peak<0.31 and RMS<0.00075 THEN	Normal
2	IF Peak ≥ 0.31 and RMS ≥ 0. 00,075 THEN	SPFO
3	IF SPFO>14.5 THEN	OF
4	IF SPFO ≤ 14.5 THEN	SPFR
5	IF SPFR>SPFI THEN	RF
6	IF SPFR ≤ SPFI	IF

Table 3
Time-domain SPs in the Training Process.

No.	State	Peak Value	RMS
1	N	0.1356	0.0002
2	N	0.0870	0.0003
3	N	0.0660	0.0003
4	IF	0.6180	0.0019
5	IF	0.6275	0.0016
6	IF	0.0629	0.0015
7	OF	1.2460	0.0013
8	OF	1.1475	0.0012
9	OF	1.1654	0.0012
10	RF	0.5847	0.0016
11	RF	0.4846	0.0017
12	RF	0.5333	0.0017

Table 4
Time-domain SPs in the Diagnosis process in turbine processors.

No.	State	Peak Value	RMS	Recognised State
1	N	0.0900	0.0004	Normal
2	N	0.1200	0.0004	Normal
3	I	1.3812	0.0004	Normal
4	I	1.6621	0.0066	Fault
5	O	1.4131	0.0036	Fault
6	O	1.2856	0.0030	Fault
7	R	0.7060	0.0025	Fault
8	R	0.7745	0.0027	Fault

veloped spectra of the fault signals processed by the SF are shown in Fig. 9. The IF and RF waveforms became clearer after noises in several frequency ranges were removed, as shown in Fig. 9(a) and (b). In particular, the waveform of the processed OF fault signal exhibited shock pulses at a regular interval, but the enveloped spectrum showed pass frequency and high-order harmonics with relatively strong noises, as shown in Fig. 9(c).

Next, during the condition survey procedure, peak value, skewness, kurtosis, and RMS SPs in the time domain were calculated [31]. The parameters (namely, peak value and RMS) of high diagnosis sensitivity were selected by the FNN as shown in Table 2, which is obtained by the FNN were implemented in MATLAB. For FNN Triangular-shaped membership functions are used for input and output variables. The membership functions are selected on a hit and trial basis with the aim of improving the classification accuracy.

The rules established by the FNN for automatically detecting fault states were peak value > 0.31 and RMS > 0.00075. In the condition survey step of the diagnosing process, there were two signal samples per state. The calculated SPs are shown in Table 3 and Table 4. Under the conditions of peak value > 0.31 and RMS > 0.00075, three signal samples were regarded as normal and five were regarded as faulty. The diagnosis results were correct.

The comparisons are carried out by the classification tools which can obtained on the internet based on MATLAB [53], and the result is shown in Table 5 and in Fig. 10. The performance of the proposed method is compared with other diagnosis methods by the experimental data for lowspeed bearing diagnosis. Signal samples from seven rotational speed categories are used. Fault bearings with outer race fault, inner race fault and roller element fault were used. Fault size is classified into "large" and "small" categories.

4. Conclusion

The fault detection of low-speed bearings is difficult to carry out using traditional diagnostic methods for high and medium speed bearings, so this paper has been conducted in an effort to establish a new diagnostic method that can be applied to intelligent diagnosis of low-speed bearings. SF, M-PH, and HT techniques are combined to extract the weak features from the vibration signals contaminated by noises, while the FNN method was used to produce rules for the automatic diagnosis. Special bearing diagnostic SPs (SSPs) were newly defined for recognition of bearing fault types, namely, SPFO, SPFR, and SPFI. In order to verify the efficiency of the proposed method, experiments were conducted on four states of bearings: normal state, inner race fault, outer race fault, and roller race fault at fixed rotational speeds of 40, 50, 60, 70, 100, 150, and 200 rpm. The results showed that as compared with those of other methods, the proposed method is considerably advantageous in terms of fault signal extraction and fault identification of low-speed bearings. The false positive and false negative rates are both 0% for distinguishing faulty state from normal state, and the accuracy rate for distinguishing fault types is 98%.

Ethical approval

This article does not contain any studies with human participants or animals performed by any of the authors.

Declaration of Competing Interest

This paper has not communicated anywhere till this moment, now only it is communicated to your esteemed journal for the publication with the knowledge of all co-authors.

References

[1] M. Cerrada, R.-V. Snchez, C. Li, F. Pacheco, D. Cabrera, J.V. de Oliveira, R.E. Vsquez, A review on data-driven fault severity assessment in rolling bearings, Mech. Syst. Signal Process. 99 (2018) 169–196.
[2] A. Glowacz, Acoustic based fault diagnosis of three-phase induction motor, Appl. Acoust. 137 (2018) 82–89.
[3] A. Glowacz, W. Glowacz, Z. Glowacz, J. Kozik, Early fault diagnosis of bearing and stator faults of the single-phase induction motor using acoustic signals, Measurement 113 (2018) 1–9 [CrossRef].

Table 5
Classify accuracies compared with proposed and existing methods.

Methods	RPM (%)						
	40	50	60	70	100	150	200
SVM	57.5	35	37.5	57.5	90	82.5	85
ANN	45	42.5	42.5	55	92.5	92.5	85
Existing Diagnosis method	100	93.75	87.5	100	100	100	100
Proposed FNN method	100	94.50	88.21	100	100	100	100

[4] L. Li, M. Chadli, S.X. Ding, J. Qiu, Y. Yang, Diagnostic observer design for TS fuzzy systems: application to real-time weighted fault detection approach, IEEE Trans. Fuzzy Syst. (2017).
[5] I. Bediaga, X. Mendizabal, A. Arnaiz, J. Munoa, Ball bearing damage detection using traditional signal processing algorithms, IEEE Instrum. Meas. Mag. 16 (2013) 20–25.
[6] L. Frosini, E. Bassi, Stator current and motor efficiency as indicators for different types of bearing faults in induction motors, IEEE Trans. Ind. Electron. 57 (2010) 244–251.
[7] M. Kang, M.R. Islam, J. Kim, J.-M. Kim, M. Pecht, A hybrid feature selection scheme for reducing diagnostic performance deterioration caused by outliers in data-driven diagnostics, IEEE Trans. Ind. Electron. 63 (2016) 3299–3310.
[8] L. Frosini, C. Harlişca, L. Szabó, Induction machine bearing fault detection by means of statistical processing of the stray flux measurement, IEEE Trans. Ind. Electron. 62 (2015) 1846–1854.
[9] N. Tandon, A. Choudhury, A review of vibration and acoustic measurement methods for the detection of defects in rolling element bearings, Tribol. Int. 32 (1999) 469–480.
[10] A.D. Nembhard, J.K. Sinha, A. Yunusa-Kaltungo, Development of a generic rotating machinery fault diagnosis approach insensitive to machine speed and support type, J. Sound Vib. 337 (2015) 321–341.
[11] A. Yunusa-Kaltungo, J.K. Sinha, A.D. Nembhard, A novel fault diagnosis technique for enhancing maintenance and reliability of rotating machines, Struct. Health Monit. 14 (2015) 604–621.
[12] M. Kang, J. Kim, L.M. Wills, J.-M. Kim, Time-varying and multiresolution envelope analysis and discriminative feature analysis for bearing fault diagnosis, IEEE Trans. Ind. Electron. 62 (2015) 7749–7761.
[13] M. Kang, J. Kim, J.-M. Kim, A.C. Tan, E.Y. Kim, B.-K. Choi, Reliable fault diagnosis for low-speed bearings using individually trained support vector machines with kernel discriminative feature analysis, IEEE Trans. Power Electron. 30 (2015) 2786–2797.
[14] K. Jiang, G. Xu, L. Liang, et al., A quantitative diagnosis method for rolling element bearing using signal complexity and morphology filtering, J. Vibro Eng. 14 (4) (2012) 1862–1875.
[15] X. Zhang, Y. Liang, J. Zhou, et al., A novel bearing fault diagnosis model integrated permutation entropy, ensemble empirical mode decomposition and optimized SVM, Measurement 69 (2015) 164–179.
[16] L. Cui, N. Wu, C. Ma, et al., Quantitative fault analysis of roller bearings based on a novel matching pursuit method with a new step-impulse dictionary, Mech. Syst. Signal Process. 68–69 (2016) 34–43.
[17] Henry Ogbemudia Omoregbee, P.S. Heyns, Fault detection in roller bearing operating at low speed and varying loads using Bayesian robust new hidden Markov model, J. Mech. Sci. Technol. 32 (9) (September 2018) 4025–4036.
[18] D.H. Pandya, S.H. Upadhyay, S.P. Harsha, ANN based fault diagnosis of rolling element bearing using time-frequency domain feature, Int. J. Eng. Sci. Technol. (IJEST) 4 (6) (June 2012).
[19] D.H. Pandya, S.H. Upadhyaya, S.P. Harsha, in: Intermittent Chaotic Behavior of High Speed Ball Bearings Due to Localized Defects, 1, Proc. 4th ICSSD, Texas A&M University (USA) & MNIT-Jaipur, India, 2012, pp. 406–413. Excel India Publishers, New Delhi, INDIA.
[20] Feng Jia, Yaguo Lei, Liang Guo, Jing Lin, Saibo Xing, A neural network constructed by deep learning technique and its application to intelligent fault diagnosis of machines, Neurocomputing 272 (2017), doi:10.1016/j.neucom.2017.07.032.
[21] M. Kang, J. Kim, J.-M. Kim, A.C.C. Tan, E.Y. Kim, B.-K. Choi, Reliable fault diagnosis for low-speed bearings using individually trained support vector machines with kernel discriminative feature analysis, IEEE Trans. Power Electron. 30 (5) (May 2015) 2786–2797.
[22] M. Kang, J. Kim, J.-M. Kim, Reliable fault diagnosis for incipient low-speed bearings using fault feature analysis based on a binary bat algorithm, Inf. Sci. 294 (Feb. 2015) 423–438.
[23] D.H. Pandya, S.H. Upadhyay, S.P. Harsha, Fault diagnosis of rolling element bearing with intrinsic mode function of acoustic emission data using APF-KNN, Expert Syst. Appl. 40 (10) (2013) 4137–4145.
[24] B. Van Hecke, J. Yoon, D. He, Low speed bearing fault diagnosis using acoustic emission sensors, Appl. Acoust. 105 (Apr. 2016) 35–44.
[25] L. Song, P. Chen, H. Wang, Automatic decision method of optimum symptom parameters and frequency bands for intelligent machinery diagnosis: application to condition diagnosis of centrifugal pump system, Adv. Mech. Eng. 6 (Nov. 2014) 603408.
[26] P. Addison, J. Walker, R. Guido, Time-frequency analysis of biosignals, IEEE Eng. Med. Biol. Mag. 28 (5) (2009) 14–29, doi:10.1109/MEMB.2009.934244.
[27] D.L. Donoho, Iain M. Johnstone, Johnstone adapting to unknown smoothing via wavelet shrinkage, J. Am. Stat. Assoc. 90 (1995) 1200–1224.
[28] B. Noda, Device for detecting damage on rotators, U.S. Patent 630 (1977) 4 007Feb. 15.
[29] S.K.Padala K.M.M. Prabhu, Systolic arrays for the discrete Hilbert transform, IEE Proc. -Circuits Devices Syst. 144 (5) (October 1997).
[30] P. Chen, in: Foundation and Application of Condition Diagnosis Technology for Rotating Machinery, Sankeisha Press, Nagoya, Japan, 2009, pp. 49–51, and 103.
[31] S. Prabhakar, A.R. Mohanty, A.S. Sekhar, Application of discrete wavelet transform for detection of ball bearing race faults, Tribol. Int. 35 (12) (2002) 793–800.

L. Mubaraali (Corresponding Author) presently working as Assistant professor in Excel Engineering College, Komarapalayam. He received his B.E Degree in Electronics and Communication Engg. from Maharaja prithivi Engineering college, Coimbatore, M.E., in VLSI DESIGN. From Regional centre ANNA UNIVERSITY, Coimbatore and Pursuing Ph.D in Information and Communication Engineering at Anna University, Chennai,

Dr. N. Kuppuswamy presently is working as Professor in Department of Mechanical Engineering KIT- Kalaignar karunanidhi institute of technology in Coimbatore,. He received his B.E Degree in Mechanical Engineering, PSG College of Technology, Coimbatore, M.E., in Production Engineering from PSG College of Technology, Coimbatore and completed Ph.D in Production Engineering. from PSG College of Technology, in 2005.

Dr. R. MuthuKumar presently working as Associate professor in Erode Sengunthar Engineering College, Erode. He received his B.E Degree in Electrical and Electronics Engg. from CIT, Coimbatore, M.E., in Power Systems Engg. From GCT, Coimbatore and completed Ph.D in Power System Engineering at Anna University, Chennai, in 2014.He has published more than eighteen international journals and has fifteen International/National conference publications. His research interest includes power system planning, voltage stability analysis and application of evolutionary algorithms to power system optimization.